Observations of day-to-day variability in precursor signatures to equatorial F-region plasma depletions

P. R. Fagundes, Y. Sahai, I. S. Batista, M. A. Abdu, J. A. Bittencourt, H. Takahashi

Ann. Geophysicae 17, 1053–1063 (1999) © EGS – Springer-Verlag 1999

Annales Geophysicae

Observations of day-to-day variability in precursor signatures to equatorial F-region plasma depletions

P. R. Fagundes[1], Y. Sahai[2], I. S. Batista[2], M. A. Abdu[2], J. A. Bittencourt[2], H. Takahashi[2]

[1] Instituto de Pesquisas e Desenvolvimento – IP&D/UNIVAP- Laboratório de Física Atmosférica e Aeronomia/LFAA – Av. Shishima Hifumi, 2911, Urbanova – São José dos Campos, SP, Brazil – CEP 12244-000
[2] Instituto Nacional de Pesquisas Espaciais – INPE – CP 515 – S.P, São José dos Campos – Brazil – CEP 12201-970

Received: 2 June 1998 / Revised: 21 October 1998 / Accepted: 14 December 1998

Abstract. In December 1995, a campaign was carried out to study the day-to-day variability in precursor signatures to large-scale ionospheric F-region plasma irregularities, using optical diagnostic techniques, near the magnetic equator in the Brazilian sector. Three instruments were operated simultaneously: (a) an all-sky (180° field of view) imaging system for observing the OI 630 nm nightglow emission at Alcântara (2.5°S, 44.4°W); (b) a digisonde (256-Lowell) at São Luis (2.6°S, 44.2°W); and (c) a multi-channel tilting filter-type zenith photometer for observing the OI 630 nm and mesospheric nightglow emissions at Fortaleza (3.9°S, 38.4°W). During the period December 14–18, 1995 (summer in the southern hemisphere), a good sequence of the OI 630 nm imaging observations on five consecutive nights were obtained, which are presented and discussed in this study. The observing period was geomagnetically quiet to moderate (Kp = 0+ to 5+; Dst = 18 nT to −37 nT). On four nights, out of the five observation nights, the OI 630 nm imaging pictures showed formations of transequatorial north-south aligned intensity depletions, which are the optical signatures of large-scale ionospheric F-region plasma bubbles. However, considerable day-to-day variability in the onset and development of the plasma depleted bands was observed. On one of the nights it appears that the rapid uplifting of the F-layer in the post-sunset period, in conjunction with gravity wave activity at mesospheric heights, resulted in generation of very strong plasma bubble irregularities. One of the nights showed an unusual formation of north-south depleted band in the western sector of the imaging system field of view, but the structure did not show any eastward movement, which is a normal characteristic of plasma bubbles. This type of irregularity structure, which probably can be observed only by wide-angle imaging system, needs more investigations for a better understanding of its behaviour.

Key words. Atmospheric composition and structure (airglow and aurora) · Ionosphere (equatorial ionosphere; ionospheric irregularities).

1 Introduction

Although equatorial spread-F irregularities have been extensively studied for about six decades since they were first reported by Booker and Wells (1938), they continue to attract considerable attention because of their strong influence on trans-ionospheric radio-wave communications. Several observational aspects, in general statistical in nature, like morphology, seasonal behaviour, altitude-longitude extent and some of the dynamical aspects of these irregularities, have been the subject of numerous investigations during the recent past and are fairly well studied (e.g. Fejer and Kelley 1980; Abdu *et al.*, 1981,1983; Maruyama and Matuura, 1984; Tsunoda, 1985; Batista *et al.*, 1986; Aarons, 1993; Sahai *et al.*, 1994; Fagundes *et al.*, 1995a, 1997; Singh *et al.*, 1997; Kil and Heelis, 1998). Large-scale equatorial ionospheric plasma depletions or bubbles, associated with equatorial range-type spread-F, are regions where the plasma densities are much lower than the ambient plasma densities and are nearly aligned along the Earth's magnetic field lines. How do precursors influence the appearance and variability of these large-scale plasma structures and their growth is still not well understood (e.g. Mendillo *et al.*, 1992; Huang *et al.* 1993) and this subject needs further investigations.

The equatorial ionospheric irregularities occur when the plasma density at the bottomside of the F-region presents a non-tilted upward gradient ∇n (where n is plasma density), so that it is antiparallel to the gravitational acceleration (**g**) and both are perpendicular to the Earth's magnetic field lines at the magnetic equator region (magnetic field lines are horizontal at the magnetic equator). Under these conditions, perturbations at the bottomside of the F-region can induce an electric field (δ**E**) which may lead to a plasma instability known as the Rayleigh-Taylor (R-T) instability. Also, a polarization electric field (**E** to eastward) at the bottomside of the equatorial F-region generates an upward $\mathbf{E} \times \mathbf{B}$

plasma drift parallel to the plasma density gradient and antiparallel to **g** and this can lead to plasma instability (Fejer and Kelley, 1980). However, the perturbations at the bottomside of the F-region can occur at any time, but the equatorial F-region irregularities or plasma bubbles are observed only during night-time (starting just after sunset) and not during daytime. The magnetic field lines at equatorial F-region heights are mapped to lower altitudes (E-region) at higher latitudes and, during the daytime, the high plasma conductivity of the E-region will suppress any electric field inhibiting the development of the plasma instability. However, after sunset, the E-region conductivity drops considerably and the electric fields generated at the bottomside of the F-region can develop plasma instabilities. The equatorial F-region irregularities have scale sizes from metres, or less, to large-scale plasma depletions, or bubbles, extending north-south to a few thousands of kilometres (aligned to the magnetic field) with east-west widths of few hundred kilometres. As recently discussed in detail by Bittencourt *et al.* (1997), the rapid uplifting of the F-region just after sunset is one of the important conditions for the onset of ionospheric plasma irregularities and fluctuations in the ion drift velocity or plasma density, caused by gravity waves or other large-scale wave structures, can act as the seed for the generation of the initial perturbation.

The equatorial plasma bubbles can be observed by both radio techniques (e.g. ionosonde, radar, scintillation etc.) and optical techniques (e.g. by observing the F-region nightglow emissions such as the OI 630 nm, OI 557.7 nm and OI 777.4 nm using either conventional photometers or wide-angle imaging systems). As discussed by Mendillo *et al.* (1997), the optical imaging of the upper atmospheric processes provides a wealth of information not available from other instruments. Also, wide-angle (180° field of view) imaging of the F-region nightglow emissions (altitude around 300 km), provides a unique diagnostic technique to observe the appearance and dynamics of equatorial plasma bubbles over regions spanning several million square kilometres. Several investigators have used wide-angle optical imaging of the F-region nightglow emissions to study large-scale equatorial plasma irregularities (e.g. Weber *et al.*, 1978; Mendillo and Baumgadner 1982; Rohrbaugh *et al.*, 1989; Mendillo *et al.*, 1992; Sahai *et al.*, 1994; Bittencourt *et al.*, 1997; Fagundes *et al.*, 1997; Taylor *et al.*, 1997; Tinsley *et al.*, 1997).

Sahai *et al.* (1994), using an all-sky OI 630 nm (this emission emanates mostly from the bottomside of the F-region by the dissociative recombination process: $O_2^+ + e \rightarrow O + O^*(^1S, ^1D)$; $O^*(^1D) \rightarrow O + h\nu$ (630 nm)) imaging system, have reported strong formation of equatorial F-region plasma bubbles during the December solstice (summer) in the Brazilian sector from observations at Cachoeira Paulista (22.7°S, 45.0°W), Brazil, a low-latitude location. Considering the fact that the equatorial F-region irregularities are generated close to the magnetic equator, it was decided to organise a campaign of observations by moving the all-sky OI 630 nm imaging system from C. Paulista to an equatorial site in Brazil at Alcântara (2.5°S, 44.4°W), during the new moon period in December 1995. The main purpose was to study the day-to-day variability in the ambient conditions that influence the appearance and growth of these large-scale disturbances. During this campaign a digisonde (256-Lowell) was operational at São Luiz (2.6°S, 44.2°W) and a multi-channel tilting-filter type zenith photometer, for observing the F-region OI 630 nm and mesospheric (OI 557.7 nm O_2 atm. (0,1) band and OH(6,2) band) emissions, was operational at Fortaleza (3.9°S, 38.4°W).

In this work we present and discuss several significant features of simultaneous ground-based optical and radio observations of large-scale equatorial F-region plasma irregularities, obtained close to the magnetic equator in Brazil during December 1995.

2 Instrumentation and observations

Observations of the OI 630 nm nightglow emission were carried out with an all-sky (180° field of view) imaging system described in detail by Mendillo and Baumgardner (1982). The system records intensified monochromatic images on 35 mm films using a conventional single lens reflex camera. Figure 1 shows the field-of-view of the imaging system with other relevant information. It should be pointed out that the imaging observation site, at Alcântara (ALC), and the ionospheric observation site, at São Luiz (SLU), are very close to each other, whereas the photometric observation site, at Fortaleza (FTZ), is about 600 km east of the other two sites. The images were recorded with 64 s exposure time. The large-scale equatorial F-region plasma depletions or bubbles, when present, are seen as quasi north-south oriented intensity depletion bands in the OI 630 nm emission all-sky images, and as the plasma bubbles

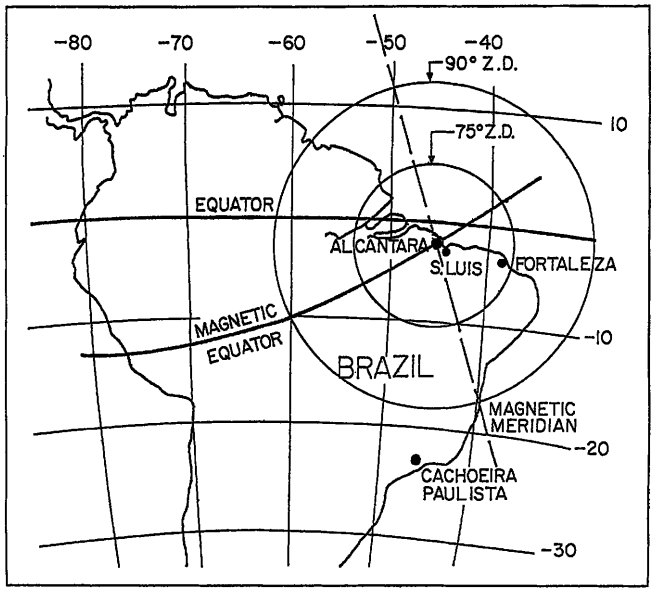

Fig. 1. The OI 630 nm emission all-sky imaging system field of view at 75° and 90° zenith angles at 300 km altitude from Alcântara

move up in the magnetic equatorial region, the depletion bands extend polewards. Also, the depletion bands are embedded in the background ionospheric plasma and, therefore, in general co-rotate with it in the eastward direction.

Notice in Fig. 2 to 5 that the images show a dark region in its southern part, which is due to the building where the radar is installed, nearby the observing site at Alcântara.

A multi-channel tilting-filter type zenith photometer is in routine operation at Fortaleza, for observing the OI 630 nm, OI557.7 nm O_2A (0,1) band at 864.5 nm, NaD 589.3 nm and OH (6,2) band at 834.37 nm nightglow emissions. The photometer characteristics have seen presented by Takahashi *et al.* (1989). It takes about 3 min to complete a full sequence of observations. The nocturnal intensity variations of the OI 630 nm emission and other simultaneous mesospheric emissions, presented, were observed during the campaign at Fortaleza.

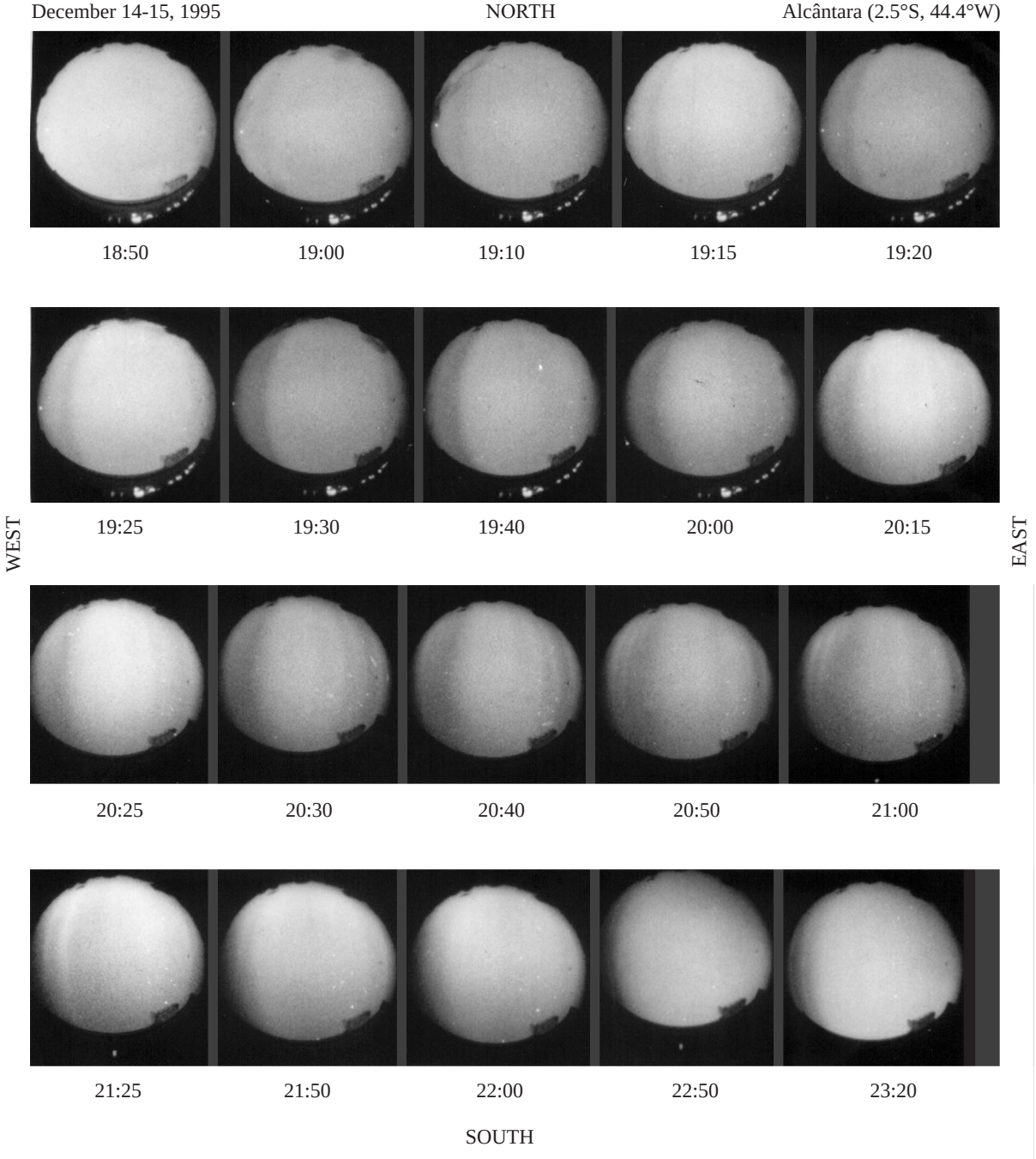

Fig. 2. Sequence of the OI 630 nm all-sky images obtained on December 14–15, 1995, at Alcântara (2.5°S, 44.4°W), Brazil

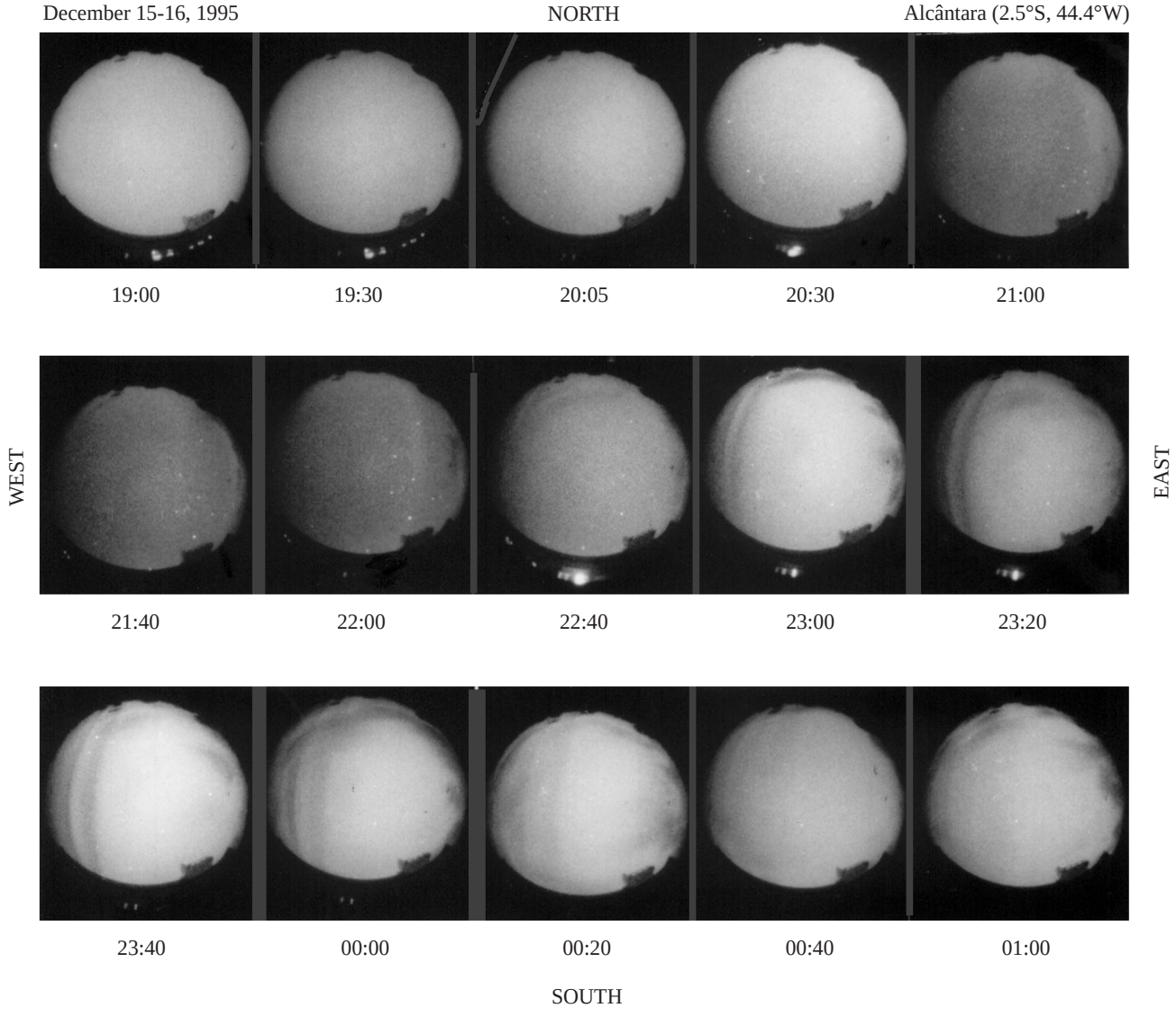

Fig. 3. Same as Fig. 3, but for December 15–16, 1995

The ionospheric sounding data (h′F and FoF2) used were recorded by a digisonde (256-Lowell) which is in routine operation at São Luiz. The ionograms are recorded at intervals of 10 or 15 min, depending on the local time (during the post-sunset enhancements of the upward $\mathbf{E} \times \mathbf{B}$ plasma drifts, ionograms are normally recorded every 10 min).

During the new moon period, in December 1995, relatively good weather conditions allowed OI 630 nm imaging observations on five consecutive nights (December 14–18) at Alcântara. However, at Fortaleza, good photometric observations were possible on only two nights i.e. December 16–17 and 17–18. The observing period was geomagnetically quiet except for the occurrence of a magnetic disturbance on December 15, with SSC occurring at 15:15 UT (12:15 LT) and attaining 3-h *Kp* maximum of 5+ during 00:00–02:00 LT, with *Dst* of −37 nT at 03:00 on December 16.

3 Results and discussion

As mentioned earlier the objective of this campaign close to the magnetic equator was to identify precursor signatures for day-to-day variability in the appearance and growth of the large-scale equatorial plasma depletions or bubbles, via OI 630 nm imaging. Table 1 presents a summary of the observing conditions and some of the main results. A perusal of Table 1 clearly indicates that considerable day-to-day differences in the appearance and growth of the equatorial irregularities do exist.

The local time variations of the ionospheric parameters (h′F and *f*oF2), observed during the campaign, are shown in Fig. 6. On December 14–15, the F-region presented a relatively small post-sunset $\mathbf{E} \times \mathbf{B}$ upward plasma drift. The h′F moved from 235 km altitude (17:30 LT) to 275 km altitude (19:00 LT). Neglecting

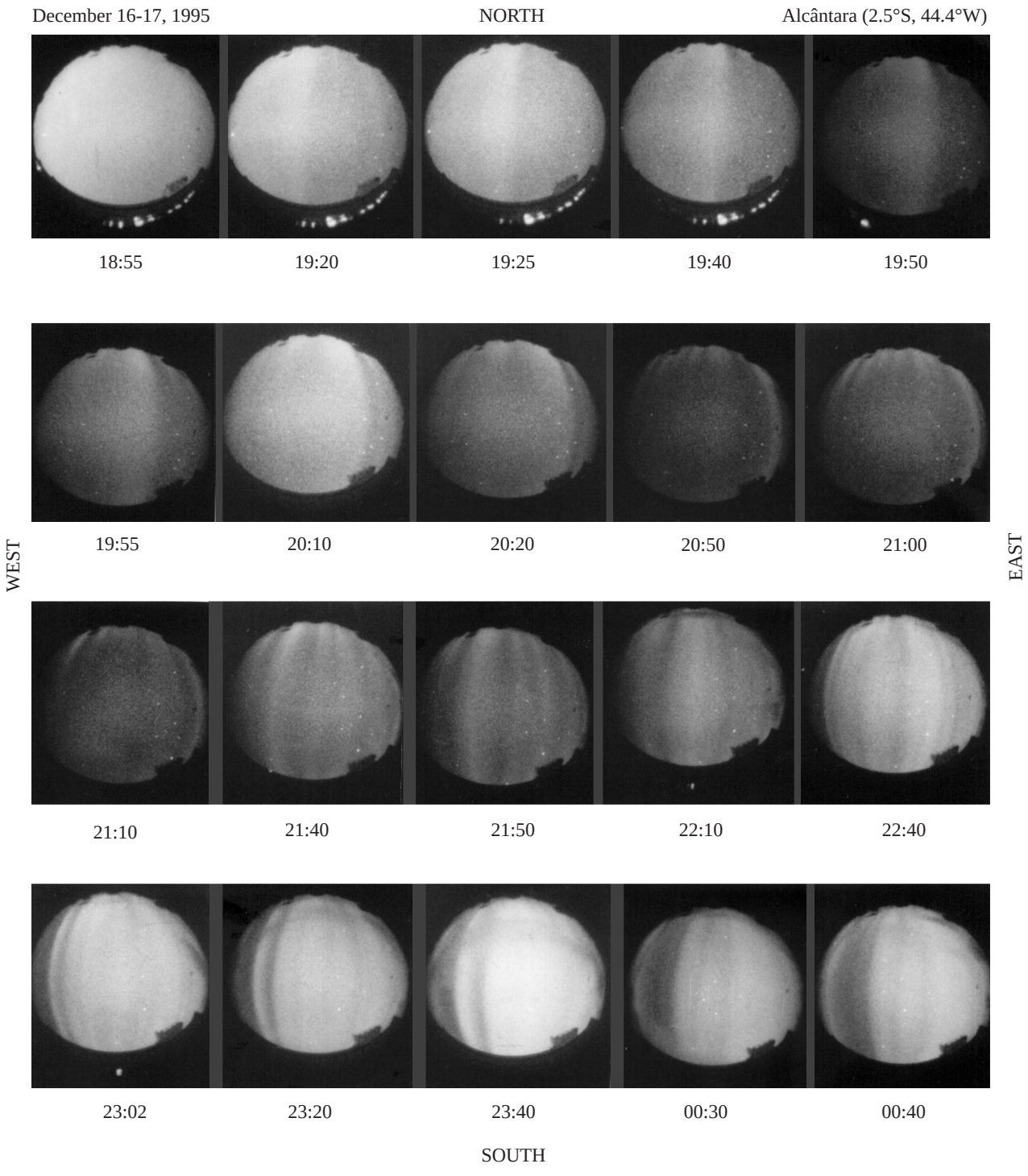

Fig. 4. Same as Fig. 3, but for December 16–17, 1995

the effects of recombination and subtleties in identifying ionogram-derived velocities with the guiding-center velocity of the plasma (e.g. Fejer *et al.* 1996), as the principal objective was to see the influence of the day-to-day variability in the upward plasma drift around the pre-reversal periods, the vertical velocity derived from the time rate of change of virtual heights during the period mentioned above was 26 km/h. The sequence of the OI 630 nm emission images obtained during the early part of this night (18:50 LT–23:20 LT), shown in Fig. 2, exhibits development of a north-south region of low intensity (depletion) at 19:20 LT,

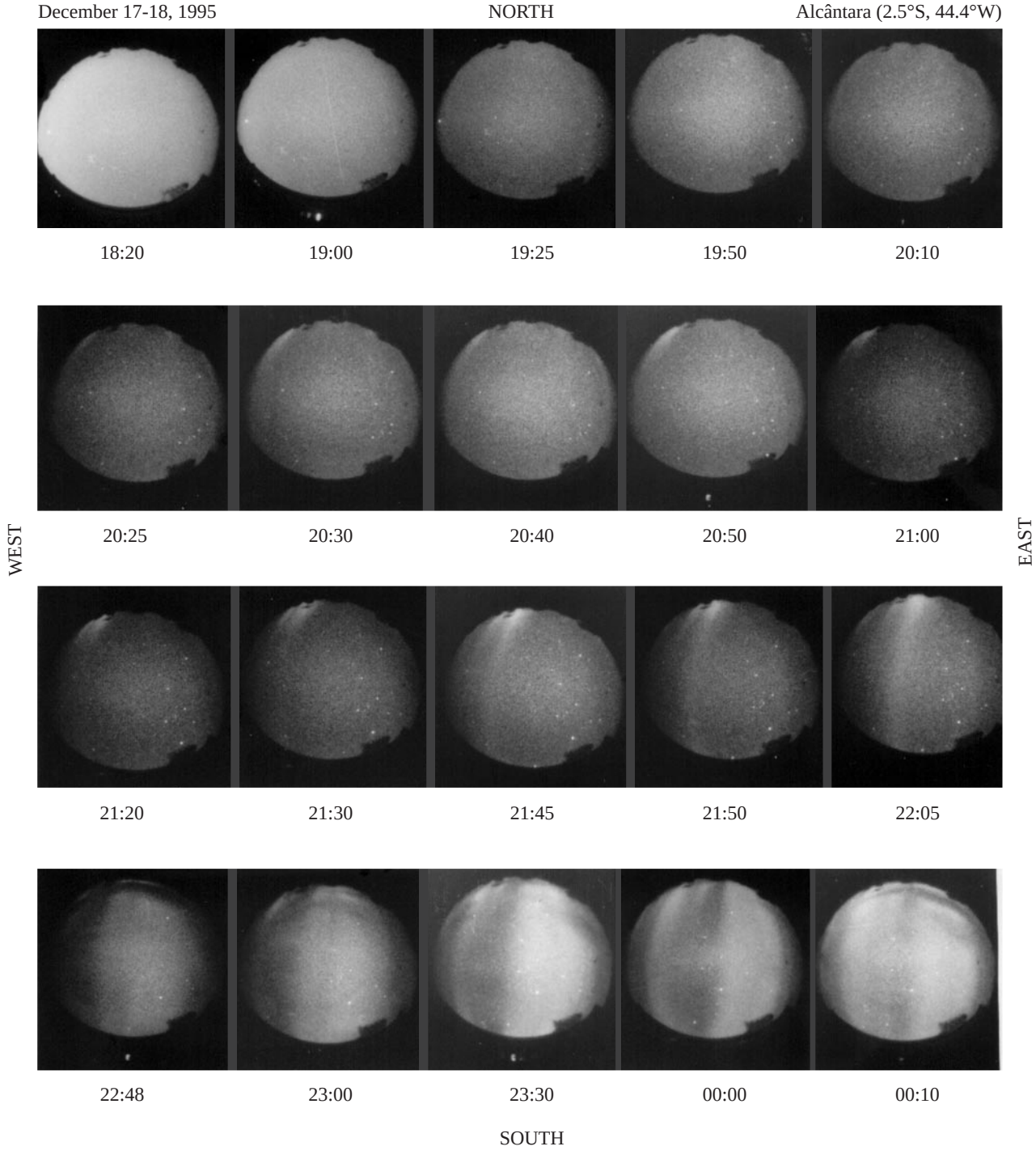

Fig. 5. Same as Fig. 3, but for December 17–18, 1995

but does not show any eastward movement in the subsequent images for more than 1 hour. This characteristic is not typical of plasma bubbles, as they normally move eastward embedded in the background plasma. Also, as shown in Table 1, the ionospheric data obtained at the very close station at São Luiz, indicated presence of only weak to moderate spread-F during this part of the night. There is no mention of this type of plasma irregularity in the literature and more routine observations of simultaneous wide-angle F-region imaging and ionospheric sounding will be important, as the appearance of more cases may allow a better understanding of the nature of these irregularities.

Table 1. Summary of observing conditions and some results

Date December 1995	Geomagnetic conditions	Mesospheric observations (Fortaleza)	Ionospheric data (São Luiz)		OI 6300 Imaging observations (Alcântara) North-south structures (n-s)	Remarks
			Pre-reversal conditions	Range spread-F conditions (LT)		
14–15	Quiet	No data	Rise rate: 26 km/h Maximum altitude reached: 275 km (19:00 LT)	Yes, 19:40–05:00; weak to moderate up to 01:15	No typical plasma bubble structures observed.	On this night, between 19:15–22:20 LT, a n-s aligned region of low intensity in the western side of the images was observed. The structure did not show the characteristic eastward movement.
15–16	Disturbed SSC 15:15 UT	No data	Rise rate: 12 km/h Maximum altitude reached: 280 km (20:30 LT)	Yes, 20:15–23:00; 03:30–05:00; weak to moderate	At 22:40 LT n-s structures formed west of the observing site, moved in the FOV and drift eastward.	No overhead formation of n-s structures.
16–17	Quiet	Shows presence of gravity-waves throughout the night.	Rise rate: 48 km/h Maximum altitude reached: 320 km (18:30 LT)	Yes, 19:15–05:00; mostly strong	Formation of n-s structures are seen at 19:40 LT and structures continue throughout of night in the FOV.	Strong overhead formation of n-s structure.
17–18	Quiet	Possibly gravity waves only in the later part of the night.	Rise rate: 75 km/h Maximum altitude reached: 400 km (20:00 LT)	Yes, 19:45–04:00; mostly strong	Formation of n-s structures are seen at 20:40 LT. However stronger structures seen much later (~23:00 LT).	Although rise rate and maximum altitude reached in this night was more rapid and higher, respectively, compared with December 16–17, the large-scale plasma structures are weaker.
18–19	Quiet	No data	Rise rate: 66 km/h Maximum altitude reached: 350 km (19:30)	Yes, 19:25–05:30; mostly strong	A typical night showing both overhead formation and drifting of n-s structures from west.	Characteristics very similar to the night of December 16–17.

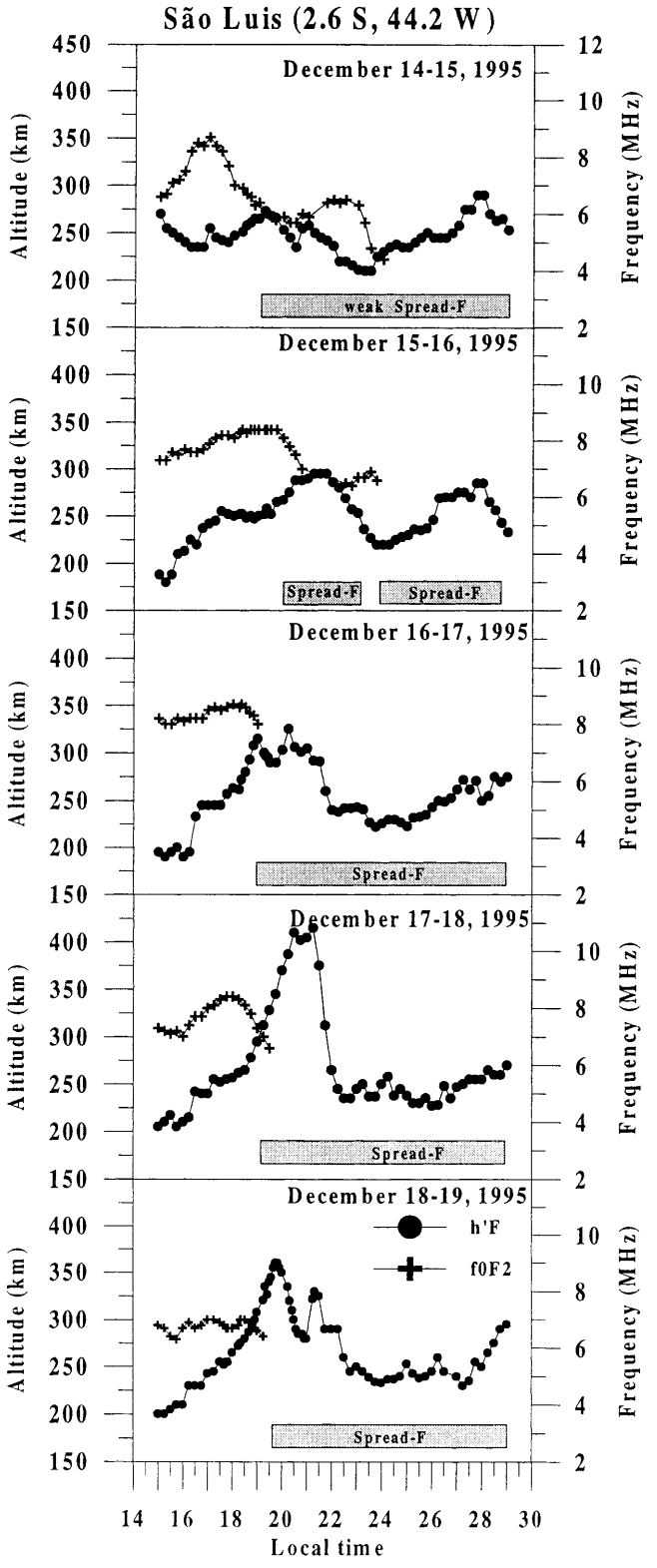

Fig. 6A–E. Local time variations of the ionospheric parameters h′F and *f*oF2 obtained at São Luis (2.6°S, 44.2°W) for all nights during this campaign: **A** December 14–15, 1995; **B** December 15–16, 1995; **C** December 16–17, 1995; **D** December 17–18, 1995 and **E** December 18–19, 1995

The local time variations of the ionospheric parameters h′F and *f*oF2, for December 15–16, are shown in Fig. 6. As mentioned earlier, a magnetic storm with SC occurred at 12:15 LT on December 15. Notice, from Table 1, that the vertical velocity around sunset time on this day is only 12 km/h, which is the lowest for the period of this campaign. Also, the ionospheric sounding data show only the presence of weak to moderate spread-F. The sequence of OI 630 nm images (Fig. 3) did not show any overhead formation of north-south aligned intensity depleted regions in the early part of the night (up to about 23:00 LT). Thereafter, some fossil plasma bubbles, formed west of the observing site moved into the field of view of the imaging system and then moved eastward. Aarons (1991) has discussed in detail the generation or inhibition of equatorial F layer irregularities during magnetic storms. However, the present case seems to indicate that there are longitudinal gradients present in the post-sunset $\mathbf{E} \times \mathbf{B}$ plasma drifts at close locations. Whether this is related or not to magnetic disturbances needs further investigations.

The local time variations of the ionospheric parameters h′F and *f*oF2, for December 16–17, are shown in Fig. 6. On this night, during the time interval from 16:00 LT to 18:30 LT, the rise of the F-layer bottomside presented an average vertical velocity of 48 km/h. The sequence of OI 630 nm images, obtained during this night (Fig. 4), shows, a very strong overhead formation and development of equatorial plasma bubbles. At 19:50 LT, the over-all intensity levels are lower compared with the earlier images and around this time the F-layer reached its maximum altitude (the OI 630 nm emission intensities are anti-correlated with the F-layer heights). Soon after the F-region attains the maximum height, the onset of spread-F event is observed (Fig. 6) and the OI 630 nm images show north-south aligned intensity depleted regions, which appear very clear in the images after 21:00 LT, when the F-layer has come to lower heights.

Fagundes *et al.* (1995b) showed that it is possible to study gravity wave activity at the mesospheric region by observing the night-time variation of the emissions (OI5577, O_2b(0,1), OH(9,4), NaD) which comes from mesospheric region. Fagundes *et al.* (1995b) observed waves with vertical wavelengths from 15 km to 70 km and vertical phase propagation velocity varying between 18 to 36 km/h, from observations carried out from 23°S in this region.

Figure 7 (December 16–17 and 17–18) shows the night-time variation of the OI 630 nm, OI557.7 nm (mesospheric component; the F-region component of the OI 557.7 nm emission was taken out from simultaneous OI 630 nm measurements), O_2 (0,1) band and OH (6,2) band intensities variations observed at Fortaleza by the zenith photometer. It is observed that the mesospheric emissions night-time variations (OI5577, O_2b(0,1) and OH (6,2) presented in Fig. 7 are similar to those presented and discussed by Fagundes *et al.* (1995b). The large intensity depletions in the OI 630 nm emission are associated with the equatorial plasma bubbles as they move across the field of view of the photometer (Sahai *et al.*, 1981). All the mesospheric

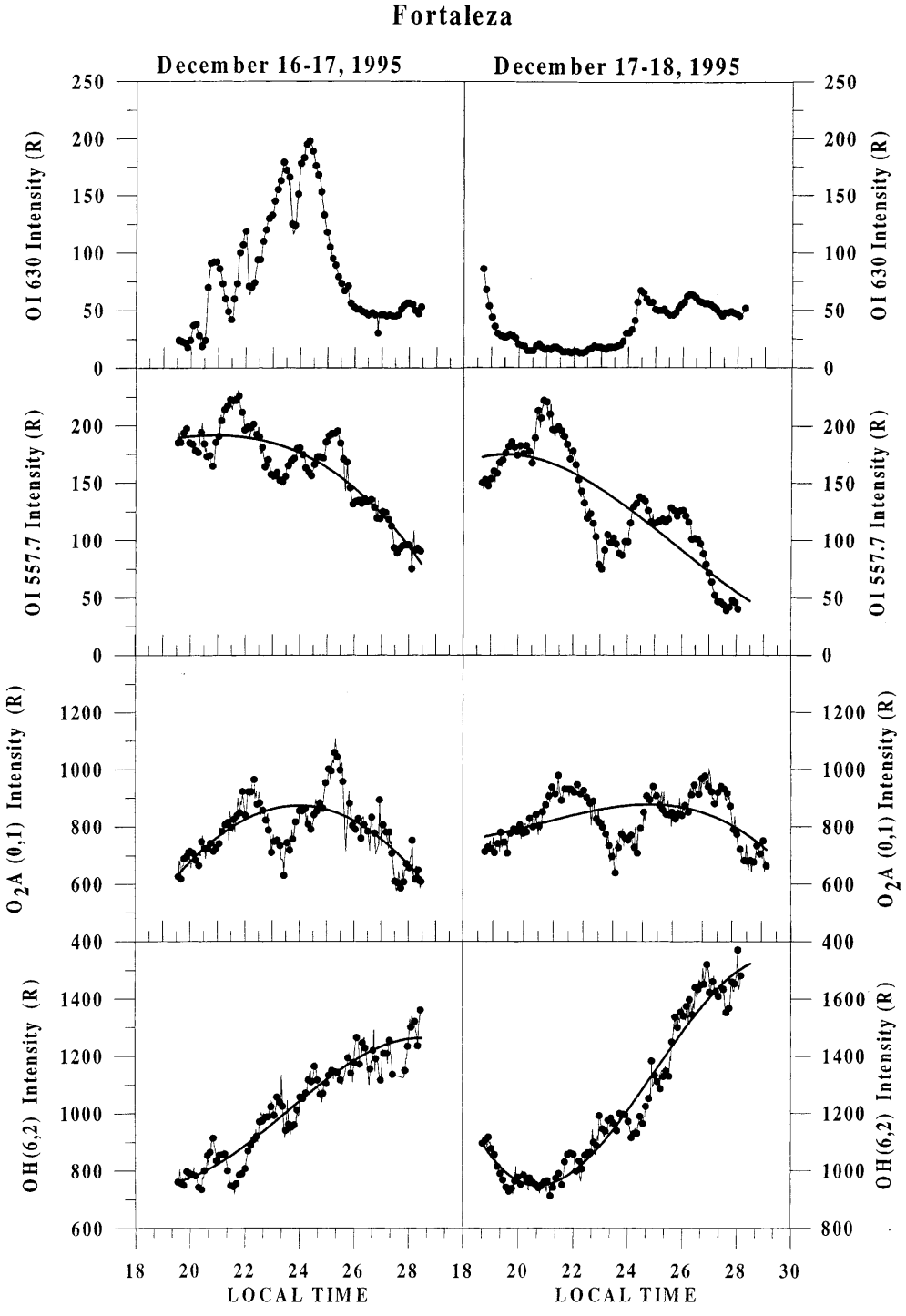

Fig. 7. Nocturnal intensity variations of the OI 630 nm emission observed on December 16–17, 1995 and December 17–18, 1995, at Fortaleza (3.9°S, 38.4°W), along with other mesospheric emissions (*continuous line* shows the night-time variation, excluding the short period fluctuations; Fagundes *et al.*, 1995b)

emissions, on the night December 16–17 (Fig. 7), show very intense gravity wave activity, particularly the OH (6,2) band emission at 87 km altitude at Fortaleza, and it is possible that the regions around it, including São Luiz and Alcântara, had strong mesospheric gravity wave activity on this night. As pointed out by Kelley *et al.* (1981), if gravity waves are responsible for seeding spread-F, they must have sources either in the auroral zone (magnetic disturbances) or in the lower atmosphere (presumably in the troposphere). Therefore, it appears that the uplifting of the F-layer, in conjunction with the propagation of the wave disturbances from the lower atmosphere, resulted in the strong spread-F observed on this night.

Figure 6 shows the local time variations of the ionospheric parameters h′F and *f*oF2 for December 17–18. It is observed that this day showed the strongest post-sunset $\mathbf{E} \times \mathbf{B}$ vertical plasma drift observed during the campaign and the average vertical velocity between 18:00 LT and 20:00 LT of the bottomside of the F-layer was about 75 km/h. The sequence of images of the OI 630 nm emission for this night is presented in Fig. 5.

However, on this night, only after 23:00 LT, it was possible to clearly see north-south aligned intensity depleted regions moving towards the east. In the earlier part of the night the F-layer is at very high altitudes and, consequently, the OI 630 nm images show very low over-all intensity levels. Also, the OI 630 nm emission intensities at Fortaleza (Fig. 7) show very low levels in the early part of the night. However, the data presented in Table 1 show the presence of strong spread-F from the time the F-layer was still moving towards the maximum altitude it reached on this day. It is, therefore, evident from these simultaneous digisonde and all-sky imaging observations, that strong spread-F may or may not result in large-scale plasma depleted regions or bubbles. It is possible that sometimes there are strong irregularity structures in the equatorial F-region after the sunset time, but these are not in the form of transequatorial plasma bubbles. Also, Fig. 7 shows that, on this night at the instability starting time, no gravity wave activity can be seen (some activity is seen but only after midnight). Therefore, it seems that the absence of the seed perturbation in this night, although with strongest post-sunset uplift, resulted in a rather less intense generation of equatorial plasma irregularities.

The characteristics of the observations on December 18–19 (Fig. 6 and Table 1) are very similar to those on December 16–17. Unfortunately, we do not have the airglow observations available from Fortaleza on this night, in order to consider the influence of gravity waves from the lower atmosphere on the initiation of equatorial spread-F.

The foregoing results and analysis do show very clearly that there is a day-to-day variability in precursor signatures to equatorial F-region plasma depletions, even during a short period of an observation campaign.

4 Conclusions

The results presented were obtained at Alcântara (2.5°S, 44.4°W), São Luiz (2.6°S, 44.2°W) and Fortaleza (3.9°S, 38.4°W), during the new moon period in December 1995, in Brazil, using two optical instruments i.e. all-sky imaging of the OI 630 nm emission and multi-channel airglow (F-region and mesosphere) photometer and a digisonde. The main features observed can be summarized as follows:

1. During the December solstice there was a strong spread-F activity in the equatorial region in the Brazilian sector, with intense plasma bubbles activity observed on four, out of five, nights of observations. The other night presented an unusual north-south intensity depleted region in the western sector without the normal eastward movement.
2. Strong spread-F activities, seen on ionograms, are not always associated with plasma bubbles, whereas plasma bubbles, as seen on the imaging system, are always associated with strong spread-F.
3. Large day-to-day variability in precursor signatures have been observed.
4. One of the nights, with the occurrence of marked post-sunset $\mathbf{E} \times \mathbf{B}$ upward plasma drift in conjunction with gravity waves from the lower atmosphere (as evidenced from mesospheric nightglow emissions), showed strong plasma bubble formation overhead the observing site, whereas another night with much stronger $\mathbf{E} \times \mathbf{B}$ upward plasma, but without mesospheric gravity wave activity, did not show marked plasma bubble formation.
5. The last remark corroborates the idea that strong and rapid post-sunset upward plasma drift is one of the important factors in the generation of equatorial ionospheric plasma bubbles, but at the same time points out to the importance of seed perturbation, which in the present investigation seems to be gravity waves from the lower atmosphere.

We plan to carry out, over an extended period, simultaneous wide-angle imaging observations of the F-region and mesospheric emissions, with ionospheric sounding and thermospheric temperature and wind measurements in the Brazilian equatorial region, in an effort to produce comprehensive databases in order to further investigate this subject.

Acknowledgements. We would like to thank Prof. Michael Mendillo from Boston University, USA, for his kind and continued interest in this bilateral research project. This work was supported by FAPESP grant 97/00810-8.

Topical Editor D. Alcaydé thanks two referees for their help in evaluating this paper.

References

Aarons, J., The role of the ring current in the generation or inhibition of equatorial F layer irregularities during magnetic storms, *Radio Sci.*, 26(4) 1131–1149, 1991.

Aarons, J., The longitudinal morphology of equatorial F-layer irregularities relevant to their occurrence, *Space Sci. Rev.*, **63,** 209–243, 1993.

Abdu, M. A., J. A. Bittencourt, and I. S. Batista, Magnetic declination control of the equatorial F-regions dynamo electric field development and spread-F, *J. Geophys. Res.*, **86,** 11 443–11 446, 1981.

Abdu, M. A., R. T. Medeiros, J. H. A. Sobral, and J. A. Bittencourt, Spread F plasma bubble vertical rise velocities determined from spaced ionosphere observations, *J. Geophys. Res.*, **88,** 9197–9204, 1983.

Batista, I. S., M. A. Abdu, and J. A. Bittencourt, Equatorial F region vertical plasma drifts: seasonal and longitudinal asymmetries in the american sector, *J. Geophy. Res.*, **91,** 12 055–12 064, 1986.

Bittencourt, J. A., Y. Sahai, P. R. Fagundes, and H. Takahashi, Simultaneous observations of equatorial F-region plasma depletions and thermospheric winds, *J. Atmos. Terr. Phys.* **59,** 1049–1059, 1997.

Booker, H. G., and H. W. Wells, Scattering of radio waves by the F-region of the ionosphere, *J. Geophys. Res.*, **43,** 249–256, 1938.

Fagundes, P. R., Y. Sahai, J. A. Bittencourt, and H. Takahashi, Relationship between generation of equatorial F-region plasma bubbles and thermospheric dynamics, *Adv. Space Res.*, **16,** 117–120, 1995a.

Fagundes, P. R., H. Takahashi, Y. Sahai, and D. Gobbi, Observation of gravity waves from multispectral mesospheric nightglow emission observed at 23°S, *J. Atmos. Terr. Phy.*, **57(4),** 395–405, 1995b.

Fagundes, P. R., Y. Sahai, I. S. Batista, M. A. Abdu, J. A. Bittencourt, and H. Takahashi, Vertical and zonal equatorial F-region plasma bubble velocities determined from OI 630 nm nightglow imaging, *Adv. Space Res.*, **20(6),** 1297–1300, 1997.

Fejer, B. G., and M. C. Kelley, Ionospheric irregularities, *Rev. Geophys. Space. Phys.*, **18,** 401–454, 1980.

Fejer, B. G, E. R. de Paula, L. Scherliess, and I. S. Batista, Incoherent scatter radar, ionosonde, and satellite measurements of equatorial F region vertical plasma drifts in the evening sector, *Geophys. Res. Lett.*, **23,** 1733–1736, 1996.

Huang, C. H., M. C. Kelley, and D. L. Hysell, Nonlinear Rayleigh-Taylor instabilities, atmospheric gravity waves and equatorial spread F, *J. Geophys. Res.*, **98,** 15 631–15 642, 1993.

Kelley, M. C., M. F. Larsen, C. Lahoz, and J. P. McClure, Gravity wave initiation of equatorial spread F: a case study, *J. Geophys. Res.*, **86,** 9087–9100, 1981.

Kil, H., and R. A. Heelis, Global distribution of density irregularities in the equatorial ionosphere, *J. Geophys. Res.*, **103,** 407–417, 1998.

Maruyama, T., and N. Matuura, Longitudinal variability of annual changes in activity of equatorial spread-F and plasma bubbles, *J. Geophys. Res.*, **89,** 10 903–10 912, 1984.

Mendillo, M., and J. Baumgardner, Airglow charcteristics of equatorial plasma depletions, *J. Geophys. Res.* **87,** 7641–7652, 1982.

Mendillo, M., J. Baumgardner, P. Xiaoqing, and J. Sultan, Onset condictions for Equatorial spread F, *J. Geophy. Res.* **97,** 13865–13876, 1992.

Mendillo, M., J. Baumgardner, M. Colerico, and D. Nottingham, Image science contributions to equatorial aeronomy: initial results from the MISETA program, *J. Atmos. Terr. Phys.*, **59**(13), 1587–1599, 1997.

Rohrbaugh, R. P., W. B. Hanson, B. A. Tinsley, B. L. Cragin, and J. P. McClure, Images of transequatorial bubbles based on field-aligned airglow observations from Haleakela in 1984–1986, *J. Geophys. Res.*, **94,** 6737–6770, 1989.

Sahai, Y., J. A. Bittencourt, N. R. Teixeira, and H. Takahashi, Plasma irregularities in the tropical F-region detected by OI 7774Å and OI 6300Å nightglow measurements, *J. Geophys. Res.*, **86,** 3496–3500, 1981.

Sahai, Y., J. Aarons, M. Mendillo, J. Baumgardner, J. A. Bittencourt, and H. Takahashi, OI 630 nm imaging observations of the equatorial plasma depletions at 16°S dip latitude, *J. Atmos. Terr. Phys.*, **56,** 1461–1475, 1994.

Singh, S., F. S. Johnson, and R. A. Power, Gravity wave seeding of equatorial plasma bubbles, *J. Geophys. Res.* **102,** 7399–7410, 1997.

Takahashi, H., Y. Sahai, B. R. Clemesha, D. Simonich, N. R. Teixeira, R. M. Lobo, and A. Eras, Equatorial mesospheric and F-region airglow emissions observed from 4° south, *Planet. Space Sci.*, **37,** 649–655, 1989.

Taylor M. J., J. V. Eccles, J. LaBelle, and J. H. A. Sobral, High resolution OI (630 nm) image measurements of F-region depletion drifts during the Guara campaign, *Geophys. Res. Lett.* **24,** 1699–1702, 1997.

Tinsley, B. A., R. P. Rohrbaugh, W. B. Hanson, and A. L. Broadfoot, Images of transequatorial F region bubbles in 630 and 777 nm emissions compared with satellite measurements, *J. Geophys. Res.*, **102,** 2057–2077, 1997.

Tsunoda, R. T., Control of the seasonal and longitudinal occurrence of equatorial scintillation by the longitudinal gradient in integrated E region Pedersen conductivity, *J. Geophys. Res.*, **90,** 447–456, 1985.

Weber, E. J., J. Buchau, R. Eather, and S. B. Mende, North-south aligned equatorial airglow depletion, *J. Geophys. Res.*, **83,** 712–716, 1978.